Molecular Dynamics Simulations of the OSS2 Model for Water and Oxonium Ion Monomers, and Protonated Water Clusters

Song Hi Lee

Department of Chemistry, Kyungsung University, Pusan 608-736, Korea

Received August 24, 2001

The OSS2 (Ojäme-Shavitt-Singer 2)[L. Ojäme *et al.*, *J. Chem. Phys.* **109**, 5547 (1998)] model for the solvated proton in water is examined for H_2O, H_3O^-, $H_5O_2^+$, $H_7O_3^+$, and $H_9O_4^+$ by molecular dynamics (MD) simulations. The equilibrium molecular geometries and energies obtained from MD simulations at 5.0 and 298.15 K agree very well with the optimized calculations.

Keywords : MD simulation, Optimized calculation, OSS2 potential, Molecular geometries and energetics.

Introduction

In the study the dynamics of H^+ in water, a dissociable water model is essential to describe how water solvent molecules can participate in ionic chemistry through dissociation and reassociation of H^+ in OH^-, H_2O, and H_3O^+. Several attempts at dissociating water potentials have been made in the past, beginning with the work of Stillinger *et al.*.[1] Recently Ojäme *et al.* reported progress in the design of a family of potentials for describing $H^+(H_2O)_n$, called OSS (Ojäme-Shavitt-Singer)n (n=1-3).[2,3] The models were generated by fitting to results of *ab initio* electronic structure calculations for the $H_5O_2^-$ ion, the H_2O molecule, and the H_3O^- ion, as well as some results for the neutral water dimer. The potential models could well reproduce *ab initio* results for the $H_5O_2^+$ ion, and could provide formation energies and structures of both protonated-water and water-only clusters that agree favorably with *ab initio* calculations used the Møller-Plesset second-order perturbation method (MP2)[4] based on the restricted Hartree-Fock wave function.

It is reported that the best results were obtained using the OSS3 potential and that the OSS2 model potential also gave good results, but usually exhibited too large bond angles for water molecule.[2] When that deficiency was not a serious problem for the application at hand, the OSS2 model was a preferred choice for simulation studies, because of the faster and less elaborate computer-code implementation as compared to the OSS3 model.

In the previous paper,[5] the OSS2 model as a dissociable water model is examined for the future study of the dynamics of H^+ in water. Molecular dynamics (MD) simulations for 216 water system, 215 water + H^+ ion system, and 215 water + OH^- ion system using the OSS2 model at 298.15 K with the use of Ewald summation were carried out. The calculated O-H radial distribution functions for these systems were essentially the same and were in very good agreement with that obtained by Ojäme.[6] This result confirmed that our method to calculate the induced dipole moment at each oxygen site within the Ewald summation is valid even though our method for the Ewald summation is different from that of Ojäme.[6]

In this paper, a further examination of the OSS2 model for H_2O, H_3O^+, $H_5O_2^-$, $H_7O_3^+$, and $H_9O_4^+$ at 5.0 and 298.15 K as a dissociable water model is carried out by MD simulations. The primary purpose of this work is to investigate equilibrium molecular geometries and energies of the small molecules and compare with the optimized results.[2]

In Section II, we present the molecular models and MD simulation method. We discuss our simulation results in Section III and present the concluding remarks in Section IV.

Molecular Models and Molecular Dynamics Simulation Methods

In the OSS2 potential model, the total energy is given by

$$V_{tot}(\mathbf{r}_1, \mathbf{r}_2, \ldots, \mathbf{r}_{n_O-n_H}) = V_{el}(\mathbf{r}_1, \mathbf{r}_2, \ldots, \mathbf{r}_{n_O-n_H}) + \sum_i^{n_O}\sum_j^{n_H} V_{OH}(r_{ij}) + \sum_i^{n_O-1}\sum_{j,j>i}^{n_O} V_{OO}(r_{ij}) + \sum_i^{n_H-1}\sum_{k,k>i}^{n_H}\sum_j^{n_O} V_{HOH}(r_{ij}, r_{kj}, \theta_{ijk}). \tag{1}$$

The first term represents the total electrostatic energy,

$$V_{el}(\mathbf{r}_1, \mathbf{r}_2, \ldots, \mathbf{r}_{n_O-n_H}) = \lim_{\{\mu_1, \ldots, \mu_{n_O}\}} \Bigg[\sum_i^{n_O-1}\sum_{j,j>i}^{n_O}\frac{q_iq_j}{r_{ij}} + \sum_i^{n_H-1}\sum_{k,k>i}^{n_H}\frac{q_iq_j}{r_{ij}} + \sum_i^{n_H}\sum_j^{n_O}\frac{q_iq_j}{r_{ij}} - \sum_i^{n_O-1}\sum_{j,j>i}^{n_O}(\boldsymbol{\mu}_i\cdot\boldsymbol{T}_{ij}\cdot\boldsymbol{\mu}_j)s_{ij}^{dd}(r_{ij}) + \sum_i^{n_O-n_H} q_i\sum_{j,j>i}^{n_O}\frac{\boldsymbol{\mu}_i\cdot\boldsymbol{r}_{ij}}{r_{ij}}s_{ij}^{cd}(r_{ij}) + \frac{1}{2\alpha}\sum_j^{n_O}\mu_i^2\Bigg]. \tag{2}$$

where $\boldsymbol{r}_{ij} = \boldsymbol{r}_i - \boldsymbol{r}_j$, and $\boldsymbol{T}_{ij}$ is the dipole tensor:

$$\boldsymbol{T}_{ij} = \frac{1}{r_{ij}^3}\left[\frac{3\boldsymbol{r}_{ij}\boldsymbol{r}_{ij}}{r_{ij}^2} - 1\right]. \tag{3}$$

Here n_O and n_H are the number of oxygen and hydrogen atoms, respectively. q_i is the charge on particle i (+e for hydrogen and -2e for oxygen), μ_i is the induced dipole on oxygen i and α is its polarizability, and $S_{ij}^{cd}(r_{ij})$ and $S_{ij}^{dd}(r_{ij})$ are the electric field cutoff functions for charge-dipole and dipole-dipole interactions, respectively. The induced dipole moment at each oxygen site can be obtained self-consistently by imposing the conditions $dV_{el}/d\mu_k = 0$, $k = 1, 2, \ldots, n_O$:

$$\boldsymbol{\mu}_i = \alpha\left[\sum_{j,j\neq i}^{n_O-n_H} \frac{\boldsymbol{r}_{ij}q_j}{r_{ij}^3}S_{ij}^{cd}(r_{ij}) + \sum_{j,j\neq i}^{n_O} \frac{\boldsymbol{T}_{ij}\cdot\boldsymbol{\mu}_{ij}}{r_{ij}^3}S_{ij}^{dd}(r_{ij})\right]. \quad (4)$$

The field cutoff function is chosen to have the following form:

$$S_{ij}(r) = \frac{r^2}{r^2 + a_1 e^{-a_2 r}}, \quad (5)$$

where the different parameters a_1 and a_2 are given form $S_{OH}^{cd}(r_{ij})$, $S_{OO}^{cd}(r_{ij})$, and $S_{OO}^{dd}(r_{ij})$. These functions approach unity as the distance goes to infinity (unscreened charges) and zero as the distance goes to zero (fully screened charges).

The second and third terms of Eq. (1) represent pairwise additive potential-energies between the H and O atoms and between the O and O atoms, respectively. For the H-O pairwise interaction, the pair potential has the form of an extended Morse function:

$$V_{OH}(r) = h_1\left[\left(1 - \frac{(1-h_5)^2 e^{-h_3(r-h_2)}}{(1-h_5)^2+h_5^2} - \frac{h_5^2 e^{-h_4(r-h_2)}}{(1-h_5)^2+h_5^2}\right) - 1\right] \quad (6)$$

The formula for the O and O pairwise interaction is

$$V_{OO} = o_1 e^{-o_2 r} + o_3 e^{-o_4 r} + o_5 e^{-o_6(r-o_7)}. \quad (7)$$

In addition to the electrostatic and pairwise additive terms, the last term of Eq. (1) represents a three-body term. This term is short range and describes the interaction within H-O-H triplets. It has the form of a polynomial in O-H distances and H-O-H angles, times a cutoff function:

$$V_{HOH}(r_1, r_2, \theta) = [k_1 + k_2(\Delta r_1 + \Delta r_2) + k_3\Delta\theta + k_4(\Delta r_1^2 + \Delta r_2^2) + k_5\Delta r_1\Delta r_2 + k_6\Delta\theta^2 + k_7(\Delta r_1 + \Delta r_2)\Delta\theta + k_8(\Delta r_1^3 + \Delta r_2^3) + k_9(\Delta r_1^2\Delta r_2 + \Delta r_1\Delta r_2^2) + k_{10}\Delta\theta^3 + k_{11}(\Delta r_1^2 + \Delta r_2^2)\Delta\theta + k_{12}\Delta r_1\Delta r_2\Delta\theta + k_{13}(\Delta r_1^2 + \Delta r_2^2)\Delta\theta^2 + k_{14}(\Delta r_1^4 + \Delta r_2^4) + k_{15}\Delta r_1^2\Delta r_2^2 + k_{16}\Delta\theta^4]\, f^{Cutoff}(r_1, r_2, \theta), \quad (8)$$

where $\Delta r = r - r_o$ and $\Delta\theta = \theta - \theta_o$ with θ being the H-O-H angle. The short-range three-body cutoff function is

$$f^{Cutoff}(r_1, r_2, \theta) = \exp[-(m_1(\Delta r_1^2 + \Delta r_2^2) + m_2\Delta\theta^2 + m_3(\Delta r_1^2 + \Delta r_2^2)\Delta\theta^2)]. \quad (9)$$

Efficient implementation of geometry optimization procedure or molecular dynamics methods requires that the forces acting on the particles can be evaluated analytically. The differentiation of this expression with respect to an atom position vector $\boldsymbol{r}_i$ will give the total force acting on the site. All the potential parameters are given in Ref. 2.

We used Gaussian isokinetics[7-10] to keep the temperature of the system constant and Gear's fifth order predictor-corrector method[11,12] is adopted to solve the equation of translational motion of each atom with a time step of 2.00×10^{-16} second (0.2 fs). Since the simulated systems are a water molecule and an oxonium ion monomer, and small water clusters, we do not apply the ordinary periodic boundary condition and the minimum image convention. Also the simulated ensemble is not necessarily specified. The equilibrium properties for each system are averaged over five blocks of 200,000,000 time steps, for a total of 1,000,000,000 time steps (200 ns) for 500,000,000 time steps to reach an equilibrium state. The configuration of each ion is stored every 10 time steps for further analyses.

Results and Discussion

A. H_2O and H_3O^+. The equilibrium geometries and energies obtained from our MD simulations for H_2O and H_3O^+ at 5.0 and 298.15 K using the OSS2 model are compared in Table 1 with the optimized results.[2,6] First of all, the geometries of H_2O and H_3O^+ at 5.0 K show an excellent agreement with the optimized ones and as a result,

Table 1. Comparison of optimized results[2,6] and those obtained from our MD simulations for H_2O and H_3O^+ using the OSS2 model. Distances in Å, angles in degrees, dipole moments in Debye, and energies in atomic units. E_μ is the last term of Eq. (2)

Properties	H_2O			H_3O^+		
	Optim.	MD(T=5.0)	MD(T=298.15)	Optim.	MD(T=5.0)	MD(T=298.15)
R(OH)	0.957880	0.957919	0.959193	0.979747	0.979794	0.981375
<HOH	109.151	109.153	109.205	109.002	108.998	109.419
μ_{AVE}	3.61958	3.61936	3.61385	3.14591	3.14626	3.07963
E_{CC}	-1.87082	-1.87067	-1.86830	-2.24555	-2.24534	-2.24431
E_{CD}^{OH}	-0.20810	-0.20808	-0.20744	-0.15720	-0.15723	-0.15064
E_{OH}	0.65080	0.65070	0.64761	0.89956	0.89941	0.89412
E_{HOH}	-0.04544	-0.04543	-0.04502	-0.11446	-0.11441	-0.11343
E_μ	0.10405	0.10404	0.10372	0.07860	0.07862	0.07532
E_{total}	-1.36951	-1.36944	-1.36943	-1.53905	-1.53895	-1.53894

each energies of H_2O and H_3O^+ at 5.0 K are also in good agreement with the optimized one. The O-H distance of H_2O agrees well with the experimental result (0.957 Å)[13] and with the MP2 calculation (0.961 Å).[4] The O-H distance of H_3O^+ also agrees well with the experimental results (0.976 Å[14] and 0.986 Å[15]) and with the MP2 one (0.979 Å). But the H-O-H angles are not so well agreed with the experimental result (104.52°)[13] and with the MP2 one (104.13°). That is why Ojäme *et al.* added the dipole-three-body coupling term to the OSS2 model and developed the OSS3 model which gives the H-O-H angle as 104.27°.[2] The average induced dipole moments obtained from our MD simulations for H_2O and H_3O^+ are also in good agreement with the optimized ones.[2]

When we turn our attention to the MD simulation results for H_2O and H_3O^+ at 298.15 K, the molecular geometries and each energies are not so well reproduced the optimized results due to the thermal movement, but those results are still acceptable. Fortuitously, the total energies of H_2O and H_3O^+ at 5.0 K and 298.15 K shows a good agreement each other and agrees well with the optimized one.

B. $H_5O_2^+$. Here we do not apply the Ewald summation[16,17] for the calculation of the induced dipole moment, but the iteration method to calculate the induced dipole moment at each oxygen site used in the revised polarized (RPOL) model[18-22] for a rigid water model is applicable. In Figure 1(a), we display stereoscopic pictures of equilibrium configurations obtained from our MD simulations at 5.0 K for $H_5O_2^+$ using the OSS2 model. The equilibrium geometry and energy obtained from our MD simulations for $H_5O_2^+$ at 5.0 and 298.15 K are compared in detail with the optimized results[2,6] in Table 2. The equilibrium bond distances (O-O, O-H_1, O-H_2, and O-H_3) at 5.0 K show a good agreement with the optimized ones and the MP2 calculations (2.390, 1.197, 0.968, and 0.969 Å).[4] The equilibrium bond angles ($<OH_1O$, $<H_1OH_2$, $<H_1OH_3$, and $<H_2OH_3$) at 5.0 K also show a good agreement with the optimized ones and the MP2 calculations (173.50, 116.08, 118.06, and 108.77°). However, the discrepancy in the torsional angles with the MP2 ones (33.19 and 100.54°) is noticeable.

As a result of the excellent agreement in the molecular geometries, the average induced dipole moment and each energy calculated from our MD simulations at 5.0 K are also in excellent agreement. In general, the overall agreements of

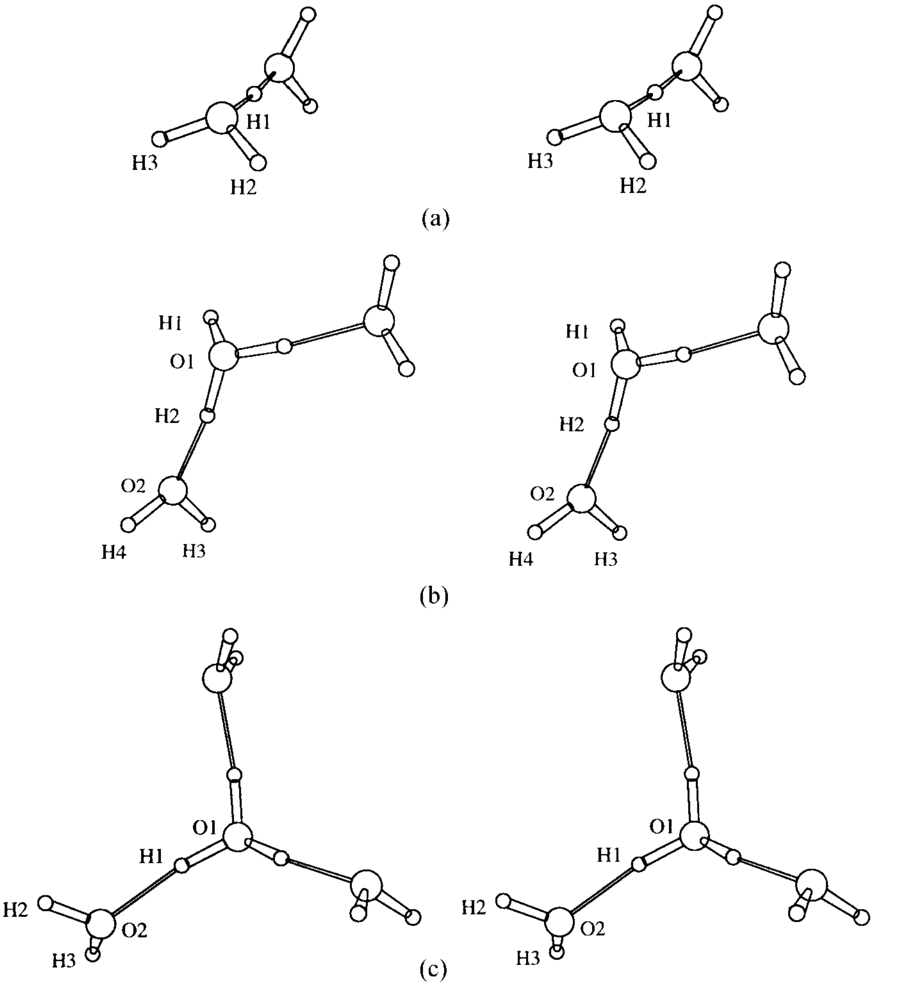

Figure 1. Stereoscopic pictures of equilibrium configurations obtained from our MD simulations at 5.0 K for (a) $H_5O_2^+$, (b) $H_7O_3^+$, and (c) $H_9O_4^+$ using the OSS2 model.

Table 2. Comparison of optimized results[2,6] and those obtained from our MD simulations for $H_5O_2^+$ using the OSS2 model. Distances in Å, angles in degrees, dipole moments in Debye, and energies in atomic units. E is the last term of Eq. (2)

		$H_5O_2^-$					
Prop.	Optim.	MD(T=5.0)	MD(T=298.15)	Prop.	Optim.	MD(T=5.0)	MD(T=298.15)
R(OO)	2.38110	2.38090	2.39550	μ_{AVE}	2.53305	2.53223	2.53735
$R(OH_1)^a$	1.19220	1.19192	1.20051	E_{CC}	-4.26877	-4.26951	-4.25707
$R(OH_2)$	0.96639	0.96653	0.96869	E_{CD}^{OH}	-0.14164	-0.14034	-0.14919
$R(OH_3)$	0.96671	0.96677	0.96869	E_{CD}^{OO}	-0.06216	-0.06160	-0.05618
$<OH_1O$	173.752	174.227	173.070	E_{DD}	-0.00002	-0.00050	-0.00138
$<H_1OH_2$	116.012	115.945	115.106	E_{OH}	1.55783^d	1.51370	1.50340
$<H_1OH_3$	115.048	114.867	115.109	E_{OO}	0.04398	0.04315	
$<H_2OH_3$	109.275	109.600	109.549	E_{HOH}	-0.14874	-0.14889	-0.14585
τ_1^b	27.970	25.796	92.182	E_μ	0.10192	0.10185	0.10286
τ_2^c	102.994	105.224	92.216	E_{total}	-2.96158	-2.96131	-2.96026

[a]H_1, the hydrogen atom between two O atoms. [b]Torsional angle of H_2-O-O'-H_2'. [c]Torsional angle of H_2-O-O'-H_3'. See Figure 1(a). [d]Sum of E_{OH} and E_{OO}.

our MD simulation results at 5.0 K with the optimized ones[2] and with the MP2[4] ones are quite good. The results at 298.15 K show somewhat poor agreement with the optimized ones due to the thermal movement, but those results are still acceptable except the torsional angles, as observed in the cases of H_2O and H_3O^+.

The H_3O^+ ion is the most stable hydrated proton species in liquid water, being slightly more stable than the C_2-symmetry structure of the $H_5O_2^+$ ion due to electronic delocalization being preferred over nuclear delocalization[23] revealed by *ab initio* calculation using 6-31G** basis set with high densities around the O atoms. A slightly more stable form of $H_5O_2^+$ involving a longer O-O distance (2.40 Å) and hydrogen bond (1.32 Å) is found to be the C_s-symmetry structure using 6-31G** basis set. The structure of $H_5O_2^+$ obtained from our MD simulations (Figure 1(a)) is close to the C_s-symmetry structure. However, other more thorough *ab initio* treatments have found the equally-spaced hydrogen-bonded structure to be the global minimum by about 0.6 kJ/mol.[24]

The presence of these three similar energy minima for the proton lying so close between the two oxygen atoms is surely the major reason for the ease of transfer of protons between water molecules: the proton moving between the extremes of triply-hydrogen bonded H_3O^+ ions ($H_9O_4^+$, 'Eigen cation') through symmetrical $H_5O_2^+$ ions ('Zundel cation').[25] When the extra proton is shared equally between more than one water molecule the approximate structure can be deduced from a consideration of the resonance structure; for example, the two shared proton in give rise to bond lengths half way between those in $(H_2O)_2$ and $H_5O_2^-$, and the three shared proton in giving rise to bond lengths a third of the way between those in $(H_2O)_2$ and $H_5O_2^+$.

C. $H_7O_3^+$ and $H_9O_4^+$. The clusters formed when adding a water molecule consecutively to the $H_5O_2^+$, $H_7O_3^-$ and $H_9O_4^-$, are shown stereoscopically in Figures 1(b) and 1(c), respectively. While the cluster geometry of $H_7O_3^-$ obtained from our MD simulations represents an oxonium ion hydrogen bonded to two water molecules with overall C_s-symmetry structure, the $H_9O_4^+$ consists of an oxonium ion coordinating three water molecules with overall C_3-symmetry structure which corresponds to the global energy minimum. There is another geometry for $H_9O_4^+$ (not shown) revealed by *ab initio* calculations,[26,27] formed by adding two water molecules to an $H_5O_2^-$ ion. It has the C_2-symmetry structure and it constitutes a local energy minimum. This geometry is never observed in our MD simulations of $H_9O_4^+$ for approximately 200 nanoseconds.

The equilibrium geometries obtained from our MD simulations at 5.0 K for $H_7O_3^-$ and $H_9O_4^+$ using the OSS2 model are compared in Table 3 with the optimized structures.[2] The geometries of $H_7O_3^+$ and $H_9O_4^+$ at 5.0 K show an excellent agreement with the optimized ones. The results at 298.15 K are not shown here since the geometry at this temperature deviates severely from the equilibrium geometry. It is worth noting that the exchange of O and H atoms within these two protonated water clusters - $H_7O_3^+$ and $H_9O_4^-$ - are occasionally observed at 298.15 K.

The two different structures of $H_9O_4^+$, the C_3-symmetry structure with a central H_3O^+ ion, $H_3O^+(H_2O)_3$, and the C_2-symmetry structure with a central $H_5O_2^+$ ion, $H_5O_2^+(H_2O)_2$,

Table 3. Comparison of optimized structures[2] and those obtained from our MD simulations for $H_7O_3^-$ and $H_9O_4^+$ using the OSS2 model. Distances in and angles in degrees

$H_7O_3^+$			$H_9O_4^-$		
Prop.[a]	Optim.	MD(T=5.0)	Prop.[b]	Optim.	MD(T=5.0)
$R(O_1O_2)$	2.471	2.4728	$R(O_1O_2)$	2.593	2.5955
$R(O_1H_1)$	0.959	0.9591	$R(O_1H_1)$	1.000	1.0002
$R(O_1H_2)$	1.036	1.0357	$R(O_2H_1)$	1.600	1.6025
$R(O_2H_2)$	1.442	1.4447	$R(O_2H_2)$	0.974	0.9747
$R(O_2H_3)$	0.970	0.9700	$R(O_2H_3)$	0.974	0.9743
$R(O_2H_4)$	0.969	0.9693	$<O_1H_1O_2$	165.18	171.419
$<O_1H_2O_2$	170.98	170.978	$<H_1O_1H_1$	114.08	114.077
$<H_1O_1H_2$	111.23	111.202	$<H_2O_2H_3$	108.66	108.672
$<H_3O_2H_4$	108.83	108.839	$\tau(O_1H_1O_3H_2)$	63.80	63.443

[a]O_1 is the central oxygen atom, H_1 is the hydrogen atom bonded to O_1 but not to O_2. H_2 is bonded to both O_1 and O_2, and H_3 and H_4 are bonded to O_2 but not to O_1. See Figure 1(b). [b]O_1 is the central oxygen atom. H_1 is the hydrogen atom bonded to both O_1 and O_2, and H_2 and H_3 are bonded to O_2 but not to O_1. See Figure 1(c).

were fully studied by the optimized calculations[2] which indicated the $H_3O^-(H_2O)_3$ form to be more stable than the $H_5O_2^-(H_2O)_2$ form by 4.1, 6.8, and 10.6 kJ/mol for OSS1-3. The MP2 calculations gave the difference between the $H_9O_4^-$ C_2 and C_3 structures as 14.8 kJ/mol.[4] The energy difference was overestimated by the restricted Hartree-Fock wave function with the 6-31G** basis set[28] and semiempirical calculations using the PM3 method[29] which gave it as 24.6 and 44.6 kJ/mol, respectively.

Concluding Remarks

In the previous paper,[5] we have examined the OSS2 water model for 216 water system, 215 water + H^+ ion system, and 215 water + OH^- ion system, and have confirmed that our method to calculate the induced dipole moment at each oxygen site within the Ewald summation is valid by a good agreement of the calculated O-H radial distribution functions for these systems with that obtained by Ojäme.[6]

In this paper, we have further examined the OSS2 model as a dissociable water model for the future study of the dynamics of H^- in water. Systems of H_2O and H_3O^-, and larger protonated water clusters - $H_5O_2^+$, $H_7O_3^-$, and $H_9O_4^+$- are studied by performing MD simulations. In general, the equilibrium geometries and energies obtained from our MD simulations at 5.0 and 298.15 K for these chemical species agree well with the optimized results.[2,6] While the cluster geometries of $H_5O_2^+$ (and $H_7O_3^-$) obtained from our MD simulations represent a proton (and an oxonium ion) hydrogen-bonded to two water molecules with overall C_s-symmetry structure, the $H_9O_4^-$ consists of an oxonium ion coordinating three water molecules with overall C_3-symmetry structure which corresponds to the global energy minimum. The C_2-symmetry structure of $H_9O_4^+$ constitutes a local energy minimum, but this geometry is never observed in our MD simulations of for approximately 200 nanoseconds. Confirming the validity of our method for the OSS2 model once more, a systematic investigation of the dissociation and reassociation of H^+ in OH^-, H_2O, and H_3O^+ is in progress.

Acknowledgment. The author thanks Prof. Y. Pak at Department of Chemistry, Pusan National University, Pusan, Korea for valuable discussions.

References

1. Stillinger, F. H.; David, C. W. *J. Chem. Phys.* **1978**, *69*, 1473; **1980**, *73*, 3384; Stillinger, F. H.; Weber, T. A. *Chem. Phys. Lett.* **1981**, *79*, 259; Weber, T. A.; Stillinger, F. H. *J. Phys. Chem.* **1982**, *86*, 1314; *J. Chem. Phys.* **1982**, *76*, 4028; **1982**, *77*, 4150.
2. Ojäme, L.; Shavitt, I.; Singer, S. J. *J. Chem. Phys.* **1998**, *109*, 5547.
3. Singer, S. J.; McDonald, S.; Ojäme, L. *J. Chem. Phys.* **2000**, *112*, 710.
4. Møller, C.; Plesset, M. S. Phys. *Rev.* **1934**, *46*, 618.
5. Lee, S. H. *Bull. Korean Chem. Soc.* **2001**, *22*, 847.
6. Private communication to Ojäme, L.
7. Gauss, K. F. *J. Reine Angew. Math.* **1829**, *IV*, 232.
8. Hoover, W. G.; Ladd, A. J. C.; Moran, B. *Phys. Rec. Lett.* **1982**, *48*, 1818.
9. Evans, D. J. *J. Chem. Phys.* **1983**, *78*, 3297.
10. Evans, D. J.; Hoover, W. G.; Failor, B. H.; Moran, B.; Ladd, A. J. C. *Phys. Rev. A* **1983**, *28*, 1016.
11. Gear, W. C. *Numerical Initial Value Problems in Ordinary Differential Equations*; McGraw-Hill: New York, 1965.
12. Evans, D. J.; Morris, G. P. *Comput. Phys. Rep.* **1984**, *1*, 297.
13. Benedict, W. S.; Gailar, N.; Plyler, E. K. *J. Chem. Phys.* **1956**, *24*, 1139.
14. Bunker, P. R.; Amano, T.; Spirko, V. *J. Mol. Spectrosc.* **1984**, *107*, 208.
15. Spirko, V.; Kraemer, W. P. *J. Mol. Spectrosc.* **1989**, *134*, 72.
16. de Leeuw, S. W.; Perram, J. W.; Smith, E. R. *Proc. R. Soc. London* **1980**, *A373*, 27.
17. Anastasiou, N.; Fincham, D. *Comput. Phys. Commun.* **1982**, *25*, 159.
18. Caldwell, J.; Dang, L. X.; Kollman, P. A. *J. Am. Chem. Soc.* **1990**, *112*, 9144.
19. Dang, L. X.; Rice, J. E.; Caldwell, J.; Kollman, P. A. *J. Am. Chem. Soc.* **1991**, *113*, 2481.
20. Dang, L. X. *J. Chem. Phys.* **1992**, *96*, 6970.
21. Dang, L. X.; Smith, D. E. *J. Chem. Phys.* **1993**, *99*, 6950.
22. Smith, D. E.; Dang, L. X. *J. Chem. Phys.* **1994**, *100*, 3757.
23. Agmon, N. *Chem. Phys. Lett.* **2000**, *319*, 247.
24. Muguet, F. F. *J. Mol. Struct. (Theochem)* **1996**, *368*, 173.
25. Marx, D.; Tuckerman, M. E.; Hutter, J.; Parinello, M. *Nature* **1999**, *397*, 601.
26. Ojäme, L.; Shavitt, I.; Singer, S. J. *Int. J. Quantum Chem., Quantum Chem. Symp.* **1995**, *29*, 657.
27. Haymet, A. D. J.; Oxtoby, D. W. *J. Chem. Phys.* **1982**, *77*, 2466.
28. Hariharan, P. C.; Pople, J. A. *Theor. Chim. Acta* **1973**, *28*, 213.
29. Srewart, J. J. P. *J. Comput. Phys.* **1989**, *10*, 209; **1989**, *10*, 221; **1990**, *11*, 543.